Kinetic study of the carbonation of epoxidized fatty acid methyl ester catalyzed over heterogeneous catalyst HBimCl-NbCl 5 /HCMC

Xiaoshuang Cai, Pasi Tolvanen, Pasi Virtanen, Kari Eränen, Jani Rahkila, Sébastien Leveneur, Tapio Salmi

Kinetic study of the carbonation of epoxidized fatty acid methyl ester catalyzed over heterogeneous catalyst HBimCl-$NbCl_5$/HCMC

Xiaoshuang Cai[1,4], Pasi Tolvanen[2], Pasi Virtanen[2], Kari Eränen[2], Jani Rahkila[3], Sébastien Leveneur[1,2*], Tapio Salmi[2]

[1]Normandie Université LSPC-Laboratoire de Sécurité des Procédés Chimiques, EA4704, INSA/Université Rouen, BP08, Avenue de l'Université, 76801 Saint-Etienne-du-Rouvray, France; E-mail: sebastien.leveneur@insa-rouen.fr

[2]Laboratory of Industrial Chemistry and Reaction Engineering, Johan Gadolin Process Chemistry Centre, Åbo Akademi University, Biskopsgatan 8, FI-20500 Åbo/Turku, Finland.

[3]Instrument Centre, Åbo Akademi University, Biskopsgatan 8, FI-20500, Åbo/Turku, Finland.

[4]College of Food Science and Technology, Henan University of Technology, Zhengzhou 450001, China.

Abstract

Carbonation of epoxidized vegetable oils is a crucial step in the preparation of non-isocyanate polyurethane. Several research groups have screened homogeneous catalysts such as tetra-n-butylammonium bromide for this reaction, but the research devoted to the use of heterogeneous catalysts and on the application of kinetic modeling is rare. Hence, to develop this process in industrial scale, an appropriate heterogeneous catalyst should be found and a kinetic model developed. A catalyst consisting of an ionic liquid supported on carboxymethyl cellulose has been proved to be a suitable heterogeneous catalyst for this carbonation reaction.

A catalyst based on 1-hydroxypropyl-3-n-butylimidazolium chloride and niobium (V) chloride supported on protonated carboxymethyl cellulose (HBimCl-$NbCl_5$/HCMC) was synthesized and tested for the carbonation of epoxidized fatty acid methyl ester. Effects of the catalyst particle size, agitation speed, catalyst loading and reaction temperature on the reaction kinetics were investigated. The carbonation reaction proceeded efficiently at a temperature of 443.15 K, agitation speed of 500 rpm, and using native catalyst particles with a median diameter of 652 μm. A kinetic model was developed to simulate the conversion of the epoxide group with time.

Keywords: Epoxidized Vegetable Oil; Carbonation; Heterogeneous Catalyst; Kinetic Modeling.

Highlights

1. Development of a process for the production of carbonated vegetable oils.
2. Shift from homogeneous to heterogeneous catalyst by using HBimCl-$NbCl_5$/HCMC.
3. Catalyst characterization of HBimCl-$NbCl_5$/HCMC.
4. Development of a kinetic model for the heterogeneously catalyzed carbonation.

1 Introduction

Global warming has become a serious political, societal and environmental issues. One of the main reasons is the well-known excess of carbon dioxide (CO_2) in the atmosphere due to exponentially increased human activities since the industrial revolution. The rapid development of human society has driven the massive demand for limited fossil resources. If the raw materials derived from fossil resources can be substituted for renewable ones such as biomass, some of the most severe environmental problems could be surmounted.[1,2] From a chemical viewpoint, CO_2 can be considered as a renewable and safe raw material. Carbon dioxide can be transformed industrially to value-added chemicals, such as urea, methanol, cyclic carbonates and some other hydrocarbon products.[3] Among all these chemicals, cyclic carbonates derived from epoxides and CO_2 are regarded as promising and feasible chemicals because they are non-toxic, eco-friendly and biodegradable. Cyclic carbonates can be used in a wide range of applications, for instance, as intermediates for polycarbonates,[4] as monomers for non-isocyanate polyurethanes,[5,6] as electrolytes for lithium ion batteries[7,8] and as synthesis materials for the manufacture of environmental polymeric coatings and resins.[9,10] Therefore, in recent years, the reaction of CO_2 with epoxidized vegetable oils (soybean oil, cottonseed oil, linseed oil, etc.), followed by the aminolysis reaction with amines to prepare non-isocyanate polyurethane, has become a highly attractive research field.[5,11,12] Carbonated vegetable oils are promising alternatives for fossil resources and have attracted particular attention. The production process is a combination of CO_2 capture and biomass valorization, both essential elements for global sustainability.[13] However, most of the research on carbonation reaction is still in laboratory-scale, rather than in industrial-scale production. The main challenge is to develop efficient catalysts and technologies to promote the carbonation reaction under moderate process conditions.[14] During the past decades, several research groups have dedicated their work to develop homogeneous and heterogeneous catalysts for the carbonation reaction. For instance, quaternary ammonium,[15] ionic liquid,[16,17] organocatalysts[18] and crown ether complexes[19] have been investigated as homogeneous catalysts. Meanwhile,

heterogeneous catalysts such as silica supported ionic liquid,[5] metal-organic frameworks,[15,20–22] and some other novel catalysts such as 2D Cu(II)-based metal-organic framework,[23] ceria-lanthana-zirconia graphene oxide (Ce-La-Zr/GO) nanocomposite catalysts,[24] carboxymethyl cellulose supported 1-hydroxypropyl-3-n-butyl limidazolium chloride and niobium (V) chloride (HBimCl-$NbCl_5$/HCMC) have been developed and tested. [22] By comparing homogeneous and heterogeneous catalytic systems, homogeneous catalysts are generally considered to have a higher catalytic activity and a higher efficiency for this reaction. Needless to say, the disadvantages of homogeneous catalysts are the complicated purification steps and insufficient catalyst recyclability, which make heterogeneous catalysts more appealing.[25]

Therefore, the current research focuses on shifting from homogeneous to heterogeneous catalysts. For instance, in 2012, Wang et al.[21] developed a solid acid catalyst $H_3PW_{12}O_{40}/ZrO_2$ for the carbonation of epoxidized soybean oil. This catalyst showed excellent efficiency but low reusability. The addition of Pt was found to improve the reusability of the catalyst. Bähr and Mülhaupt studied the carbonation of epoxidized linseed oil and epoxidized soybean oil. A homogeneous catalyst, tetra-butylammonium bromide (TBABr), and a heterogeneous catalyst, silica-supported 4-pyrrolidinopyridinium iodide (SiO_2-(I)), were applied for the reaction. It was demonstrated that a complete conversion was reached using 30 bar,140°C and 45 hours with SiO_2-(I) and 20 hours with TBABr, respectively.[5]

Cellulose is one of the most commonly used polymeric raw material because it is eco-friendly, biodegradable, sustainable and renewable.[26] Cellulose has been reported as a suitable supporting material for heterogeneous catalysts,[22,27–29] and carboxymethyl cellulose-supported ionic liquid seems to be promising as a heterogeneous catalyst. In 2012, Roshan et al.[30] reported the use of carboxymethyl cellulose supported imidazolium-based ionic liquid catalyst for the carbonation of propylene oxide. During the carbonation reaction, the catalyst displayed high activity, selectivity and excellent reusability. It was pointed out that the carboxyl and hydroxyl groups on the carboxymethyl cellulose play a synergistic role with the halide ions during the carbonation process. The carboxyl group on the carboxymethyl cellulose might

stabilize the product and promote the reaction through hydrogen bonds.[30] In 2012, Sun et al.[31] studied the carbonation of epoxides catalyzed by chitosan functionalized 1-ethyl-3-methyl imidazolium halides. As a result, the carbonation reaction achieved a high yield and a high selectivity, and the catalyst showed excellent recyclability and reusability.[31] In 2013, Tharun et al.[32] studied the carbonation of epoxides in the presence of a chitosan catalyst. The microwave-quaternized catalyst showed an excellent activity and a high selectivity (> 99 %) during solvent-free carbonation. It was also reported that a shorter alkyl chain length and more nucleophilic anion gave a higher activity.[32] In 2016, Wu et al.[22] prepared a heterogeneous catalyst, consisting of an imidazolium-based ionic liquid and Lewis acid supported on carboxymethyl cellulose. They found out that this kind of immobilized catalyst on carboxymethyl cellulose was very resistant towards leaching and showed good catalytic properties, such as excellent stability, high activity and selectivity.

Although cellulose-supported heterogeneous catalysts have been reported to catalyze the carbonation reaction, this kind of catalyst has been investigated only for epoxides of small molecular size, such as propylene oxide and styrene oxide. Reports on the use of cellulose supported heterogeneous catalysts for the carbonation of epoxidized vegetable oil are rare.

In this work, the heterogeneous catalyst HBimcl-$NbCl_5$/HCMC (carboxymethyl cellulose supported 1-hydroxypropyl-3-n-butylimidazolium chloride and niobium (V) chloride) was selected and synthesized following the guidelines of Wu et al.[22] Epoxidized fatty acid methyl ester derived from cottonseed oil was investigated for the carbonation kinetics. Cottonseed oil was chosen because it is seen as a by-product of the cotton industry and can also be upgraded to biodiesel.[33]

The influences of internal and external mass transfer on the reaction kinetics were evaluated by using different catalyst particle sizes and agitation speeds. A kinetic model was developed to estimate the rate constants of carbonation.

2 Material and methods

2.1 Materials and chemicals

Refined cottonseed oil, formic acid (purity > 99 %), acetic acid (purity > 99 %), tetraethylammonium bromide (TEAB, 98 %), solution of 0.1 mol.L^{-1} of sodium thiosulfate, 1-butylimidazole, 3-chloro-1-propanol, sodium hydroxide, phosphoric acid (purify⩾ 85 wt. % in water), sodium carboxymethyl cellulose (NaCMC) with a degree of substitution of 1.2 and niobium (V) chloride were purchased from Sigma-Aldrich (Sigma Aldrich Chemical Co, USA). Hydrogen peroxide (30 wt. % in water) solution and 0.1 mol.L^{-1} of iodine (HANUS solution) were obtained from EMSURE (Darmstadt, Germany). Standardized perchloric acid solution of 0.1 mol.L^{-1} in acetic acid was obtained from VWR International SAS (Fontenay-sous-Bois, France). Chloroform, ethyl acetate and anhydrous ethyl ester were purchased from Honeywell Riedel de Haën (Seetze, Germany). Hydrochloric acid was obtained from VWR International SAS (37 %, Fontenay-sous-Bois, France).

2.2 Synthesis of HBimCl-$NbCl_5$/HCMC

The heterogeneous catalyst HBimCl-$NbCl_5$/HCMC was prepared according to the procedure of Wu et al.,[22] with slight modifications. The procedure is described in detail here.

2.2.1 Preparation of protonated carboxymethyl cellulose (HCMC)

NaCMC (4 g) was added into 200 mL of isopropanol solution (75 vol. % in water). Then, 20 mL of HCl (37%) was added and mixed through stirring for three hours. The product was filtrated and washed with an isopropanol solution (65 vol. % in water) until no Cl^- was left in the washing solution. The Cl^- in the washing solution was tested by a silver nitrate test in a clean test tube, where 2-3 drops of silver nitrate solution (0.1 mol.L^{-1} in distilled water) were added. Then, the mixture was shaken to mix and placed in the dark place for 10 minutes before close observation. The disappearance of white precipitate indicated no Cl^- residue. After that, the solution was heating up to evaporate isopropanol and water. Compared to Wu et al.,[22] isopropanol was chosen instead of ethanol to decrease the side reaction of esterification.

2.2.2 Preparation of 1-hydroxypropyl-3-n-butylimidazolium chloride (HBimCl)

1-chlorobutane (1.29 g, 13.6 mmol) and 1-butylimidazole (98 % purity, 1.69 g, 13.6 mmol) were weighted out and mixed in a three-necked glass reactor at 100 °C for 20 hours under argon atmosphere. The product was washed three times with ethyl acetate to remove the unreacted reactant, following by evaporation to remove ethyl acetate. ^{1}H NMR was used to characterize the final product as desired (Figures S4-S5). ^{1}H NMR (500.20 MHz, $CDCl_3$, 25 °C): δ = 10.34 (s, 1 H, H-2), 7.71 (d, 1 H, $J_{H\text{-}5,\ H\text{-}4}$ = 1.2 Hz, H-5), 7.40 (d, 1 H, H-4), 5.17 (bs, 1 H, 3'-OH), 4.54 (t, 2 H, $J_{H\text{-}1',\ H\text{-}2'}$ = 6.2 Hz, H-1'), 4.31 (t, 2 H, $J_{H\text{-}1'',\ H\text{-}2''}$ = 7.3 Hz, H-1''), 3.61 (t, 2 H, $J_{H\text{-}3',H\text{-}2'}$ = 5.2 Hz, H-3'), 2.11 (tt, 2 H, H-2'), 1.91 (tt, 2 H, $J_{H\text{-}2'',\ H\text{-}3''}$ = 7.7 Hz, H-2''), 1.39 (tq, 2 H, $J_{H\text{-}3'',\ H\text{-}4''}$ = 7.4 Hz, H-3''), 0.97 (t, 3 H, H-4'') ppm. ^{13}C NMR (125.8 MHz, $CDCl_3$, 25 °C): δ = 137.6 (C-2), 122.9 (C-5), 121.7 (C-4), 58.9 (C-3'), 49.9 (C-1''), 46.9 (C-1'), 32.8 (C-2'), 32.1 (C-2''), 19.5 (C-3''), 13.5 (C-4'') ppm.

2.2.3 Preparation of HBimCl-$NbCl_5$/HCMC

The chemicals HBimCl (1.088 g, 4.88 mmol) and niobium (V) chloride (0.6704 g, 2.48 mmol) were co-dispersed in 20 mL of dimethylformamide at 100 °C for 5 hours under argon atmosphere. Then, the mixture was cooled down to 70 °C, after which 2 g of HCMC was added and stirred overnight. The resulting mixture was heating up to evaporate the solvent, followed by washing with anhydrous ethyl ether and evaporated to obtain the purified HBimCl-$NbCl_5$/HCMC.

2.2.4 Catalyst characterization

Fourier-transform infrared spectra (FTIR) were obtained by a Bruker IFS 66/s spectrometer (Bruker, Germany) in the spectroscopic range of 4000-400 cm^{-1} at 4 cm^{-1} of resolution averaging 31 scans. Thermogravimetric analysis (TGA) was performed on Cahn D-200 microbalance (Thermo Cahn, America) with a sensitivity of 1 μg within a temperature range of 20-700 °C. The heating rate was 10 °C.min^{-1} under argon atmosphere. Scanning electron microscopy (SEM, JEM 1400 plus, JEOL Ltd., Japan) coupled with an energy dispersive X-ray

analyzer was used to describe the surface topography of the sample. Inductively coupled plasma mass spectrometry (ICP-MS) was used to quantify the amount of niobium on the fresh and spent catalyst. ^{1}H and ^{13}C NMR were applied to characterize the functional groups for the catalyst and for the substances prepared during the different synthesis steps. Liquid state NMR spectra were recorded on a Bruker (Bruker BioSpin GmbH, Rheinstetten, Germany) AVANCE III spectrometer operating at 500.20 MHz (^{1}H) and 125.8 MHz (^{13}C) equipped with a Prodigy BBO CryoProbe. Characterization of small molecular compounds was carried out by a standard set of experiments, ^{1}H, ^{13}C, DQF-COSY (Double-Quantum Filtered COrrelation SpectroscopY) HSQC (Heteronuclear Single-Quantum Coherence, multiplicity edited) and HMBC (Heteronuclear Multiple-Bond Correlation). Chemical shifts are reported in ppm, with two decimals in ^{1}H and one decimal in ^{13}C, and referenced to an internal standard (TMS, $\delta_{1H} = \delta_{13C} = 0$ ppm). Coupling constants are reported in Hz with one decimal. Solid state NMR spectra were recorded on a Bruker AVANCE III spectrometer operating at 399.75 MHz (^{1}H) and 100.5 MHz (^{13}C) equipped with a CP-MAS probe. A spin-rate of 14 kHz and a contact time of 2 ms was used, and 20 k or 40 k transients were acquired for each sample.

The particle size distribution of the catalyst was measured by a Malvern Mastersizer 3000.

2.3 Preparation of fatty acid methyl ester (FAME): transesterification of cottonseed oil

The FAME was prepared, as described in the previous work.[34] The transesterification was performed in a double-jacketed glass reactor equipped with a mechanical stirrer and a reflux condenser. For that, 200 mL of methanol and 8.4 g of base catalyst sodium hydroxide were well mixed and preheated before adding into 800 mL of cottonseed oil at a constant temperature of 70 °C. The reaction lasted for one hour. After that, the glycerol phase in the lower layer was removed, while the fatty acid methyl ester left in the top layer was washed with preheated distilled water (800 mL) containing one drop of phosphoric acid (0.5 mL), and finally with pure distilled water. The purified product was heating up by an IKA RV10 control vacuum rotary evaporator at 70 °C and then dried over anhydrous magnesium sulfate followed by filtrated in a Buchner funnel through filter paper with a pore size of 25 μm.

2.4 Preparation of epoxidized fatty acid methyl ester (EFAME)

FAME (100.0 g), water (20.0 g) and H_2O_2 (150.0 g) were well mixed under 40 °C in the glass-jacketed reactor. After that, formic acid was added continuously with a feeding rate of 2.1 $mL.min^{-1}$ for 20 minutes. The overall reaction lasted for 2 hours. The organic phase was then separated and washed with 5 wt. % of Na_2CO_3 aqueous solution followed by purification with distilled water to remove the remained acid and salt. The purified product was heated at 60 °C and dried using anhydrous magnesium sulfate.

2.5 Carbonation of epoxidized fatty acid methyl ester (CFAME)

Carbonation experiments were conducted in a 300 mL high-pressure stainless-steel autoclave, as described in the previous work.[34] The reactor was equipped with a hollow-shaft gas entrainment impeller (diameter 2.5 cm), a temperature control system, gas feed and monitoring system. The accuracy given by the recorder was 0.01 bar for the pressure probe and 0.1 °C for the temperature probe. Figure 1 shows a simplified scheme of the reaction setup.

Figure 1. Simplified scheme of the reaction setup

2.6 Analysis method

Evolutions of functional groups (double bond, epoxide and carbonate group) were characterized by FTIR and by titration measurements during reaction steps.

Concentration of epoxide group

The epoxide content was determined by potentiometric titration as described by Maerker.[35] An oil sample (0.100 g) was weighted out and dissolved in 10 mL of chloroform, and then mixed with 10 mL of 20 wt. % TEAB in acetic acid. Then, the mixture was titrated by a standard solution (0.1 $mol.L^{-1}$) of perchloric acid in acetic acid. The concentration of the epoxide group was calculated from

$$[\text{Epoxide group}]\ (\text{mol.L}^{-1}) = \frac{0.1 \cdot V_{\text{titration}}}{m_{\text{sample}}/\rho_{\text{sample}}} \quad (1)$$

where $V_{titration}$ is the titration volume of the oil sample in L; m_{sample} is the mass of the measured sample in g and ρ is the oil density of the sample in g.cm^{-3}. More information was provided in Figure S1. The experimental error was measured via the standard deviation of replicate value, and was calculated to be lower than 0.15 mol/L.

Concentration of double bonds

The double bond content was titrated as described by Paquot.[36] An oil sample (0.200 g) was weighted out and dissolved in 10 mL of chloroform, followed by adding 10 mL of Hanus solution (0.1 mol.L^{-1}, iodine solution), and kept in darkness for 1 h to complete the reaction. Then, 10 mL of 10 wt. % potassium iodide solution and 100 mL of water were added and mixed before titration with 0.1 mol.L^{-1} sodium thiosulfate solution (Figure S2). The double bond concentration was calculated from

$$[\text{Double bond}]\ (\text{mol.L}^{-1}) = \frac{0.1\cdot(V_{blank}-V_{titration})}{(m_{sample}/\rho_{sample})\cdot 2} \quad (2)$$

where, V_{blank} is the titration volume of blank in L; $V_{titration}$ is the titration volume of the oil sample in L; m_{sample} is the mass of measured sample in g, and ρ is the oil density of the sample in g.cm^{-3}, 2 is the associate coefficient.

2.7 Kinetic and mass transfer experiments

The experimental matrix for kinetic modeling is displayed in Table 1. The terms [*Ep*], [*DB*] and [*Cat.*]$_0$ stand for the initial concentrations of epoxide group, double bond and catalyst, respectively.

During the kinetic study, 45.0 g of EFAME and the desired amount of catalyst were weighted out in the autoclave reactor. Then, the mixture was mixed and preheated under nitrogen atmosphere, followed by being purged with CO_2 for two times. Samples were withdrawn during the reaction via the sampling port, which was equipped with a 7 μm stainless filter and immersed in the reaction mixture.

Before the experiments, the catalyst was manually pressed and crushed and then sieved mechanically to the fractions 355-500 μm, 125-355 μm and 63-125 μm. For each fraction, the

effect of the particle size on the kinetics of carbonation was evaluated. Tables 1 and 2 display the experimental matrices for the carbonation reaction and mass transfer study, respectively. The term $[Cat.]_0$ is the amount of active site on the solid catalyst per volume of the reaction mixture.

Table 1 Experimental matrix for kinetic modeling

The mass transfer experiments were conducted as described in the previous work of our group.[34] During the mass transfer study, 90.0 g of oil sample was weighted out and preheated up to the desired temperature under nitrogen atmosphere. The reactor was purged two times with CO_2 and kept for 2-3 minutes for stabilization. As the CO_2 pressure was stabilized, the agitation was started at 500 rpm. The CO_2 pressure and temperature in the gas reservoir and the reactor were recorded. A pressure regulator was used to maintain the CO_2 pressure constant. The experimental matrix displayed in Table 2 was designed to estimate the mass transfer coefficients and Henry's constant at different temperatures and composition.

Table 2 Experimental matrix for mass transfer modeling with initial concentrations

2.8 Kinetic modeling

Based on the literature,[22] the mechanism of carbonation of EFAME can be illustrated by four steps, as shown in Figure 2.

Figure 2. Simplified mechanism of carbonation of EFAME by HBimCl-$NbCl_5$/HCMC

The overall reaction can be described as:

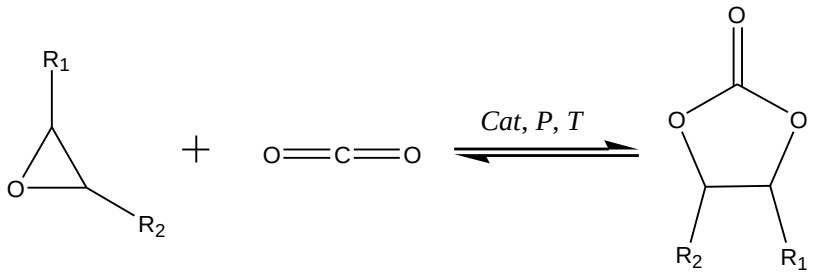

The third reaction step (iii) of the reaction was assumed to be the rate-determining. Thus, the carbonation reaction kinetics can be written as

$$R_{\text{Carbonation}} = R_3 = k_3 \cdot [I_2] \cdot [\text{CO}_2]_{\text{liq}} \quad (3)$$

The quasi-equilibrium approximation was applied to steps 1 and 2,

$$K_1 = \frac{[I_1]}{[Ep]\cdot[*]} \quad (4)$$

$$K_2 = \frac{[I_2]}{[I_1]} \quad (5)$$

where, $[I_1]$ and $[I_2]$ are the concentrations of intermediate 1 and intermediate 2, respectively and $[*]$ is the concentration of active sites at time *t*.

By combining Eq.(4) and Eq.(5), the concentration of the intermediate 2 can be expressed as

$$[I_2] = K_1 \cdot K_2 \cdot [Ep] \cdot [*] \quad (6)$$

Thus, the carbonation reaction kinetic becomes:

$$R_{\text{Carbonation}} = k_3 \cdot K_1 \cdot K_2 \cdot [Ep] \cdot [*] \cdot [\text{CO}_2]_{\text{liq}} \quad (7)$$

Therefore, mass balance applied to the surface species leads to

$$[Cat.]_0 = [*] + [I_1] + [I_2] + [I_3] \quad (8)$$

where, $[Cat.]_0$ is the initial catalyst concentration and $[I_3]$ is the concentration of intermediate 3.

By assuming that $[I_3] \sim 0$, the concentration of active sites at time *t* is

$$[*] = \frac{[Cat.]_0}{1+K_1\cdot[Ep]\cdot(1+K_2)} \quad (9)$$

The following notations are introduced: $k_{carbonation}$=K_1·K_2·K_3. and $\propto = 1 + K_1 \cdot (1 + K_2)$. Eq.(7) then becomes

$$R_{\mathrm{Carbonation}} = k_{\mathrm{Carbonation}} \cdot \frac{[Ep]\cdot[Cat.]_0\cdot[\mathrm{CO_2}]_{\mathrm{liq}}}{1+\propto\cdot[Ep]} \quad (10)$$

All the associated parameters were estimated during the kinetic modeling stage.

The material balances of the different components in this reaction system can be described by the following ordinary differential equations:

$$\frac{\mathrm{d}[EP]}{\mathrm{d}t} = -R_{\mathrm{Carbonation}} \quad (11)$$

$$\frac{\mathrm{d}[Carb]}{\mathrm{d}t} = R_{\mathrm{Carbonation}} \quad (12)$$

$$\frac{\mathrm{d}[\mathrm{CO_2}]}{\mathrm{d}t} = -R_{\mathrm{Carbonation}} + (k_{L.}a) \cdot ([\mathrm{CO_2}]^*_{\mathrm{liq}} - [\mathrm{CO_2}]_{\mathrm{liq}}) \quad (13)$$

where, $(k_{L.}a) \cdot ([\mathrm{CO_2}]^*_{\mathrm{liq}} - [\mathrm{CO_2}]_{\mathrm{liq}})$is the gas-liquid mass transfer of CO_2, mol.L^{-1}.s^{-1}; $k_{L.}a$ is the overall mass transfer of CO_2 in the liquid phase and $[\mathrm{CO_2}]^*_{\mathrm{liq}}$ is the equilibrium concentration of CO_2 in the gas-liquid phase, mol.L^{-1}. The estimation of $k_{L.}a$ was done in the same way as in the previous articles of our group.[34,37] The details of the modeling results can be found in the Supporting Information (Figures S8-S9 and Table S1).

During the kinetic modeling stage, the concentration of the epoxide group was used as observable. The modeling was performed by using ModEst software, written in Fortran 90.[38] The system of ordinary differential equations (ODEs) was solved by the ODESSA algorithm, which is a package of Fortran routines based on backward difference method.[39]

The coefficient of determination θ^2 is one of the most common measures to evaluate the goodness of a data fitting and is defined as:

$$\theta^2 = 1 - \frac{(y_i-\hat{y}_i)^2}{(y_i-\bar{y})^2} \quad (14)$$

where, $\hat{y}_i$ is the observable simulated by the model, $\bar{y}$ is the mean value of the experimental observables and y_i is the experimental observable. The standard error of the estimated parameter represents 95 % of the confidence interval. The objective function f was

$$f = \sum(y_i - \hat{y}_i)^2 \quad (15)$$

The objective function was firstly minimized by the simplex algorithm,[40] using arbitrary initial guess values when the knowledge of the initial guess values was unknown. After that, the Levenberg-Marquardt algorithm was used to improve the parameter estimation.[41]

3 Results and discussion

3.1 Catalyst characterization

Figure 3 shows the solid state ^{13}C NMR spectra of the three polymeric compounds NaCMC (A), HCMC (B) and HBimCl-$NbCl_5$/HCMC (C). The carboxyl peak at 176 ppm in NaCMC shifted to 172 ppm in HCMC as expected.[22] The peaks at 125 ppm and 135 ppm were from the imidazole moiety,[42] and the signals between 10 and 50 ppm assigned to aliphatic chains connected to the imidazole,[43] where peaks did not appear in NaCMC (A) and HCMC (B) due to the fact that the functionalized imidazole was not present. The peaks between 50 and 110 ppm assigned to the cellulose backbones, and the peaks between 160 to 175 ppm correspond to the carboxylic acids.

The content of carboxyl groups in the final protonated carboxymethyl cellulose was calculated as 4.88 ± 0.01 $mmol.g^{-1}$. The details are reported in the Supporting Information.

Figure 3. ^{13}C CP-MAS spectra of NaCMC (A), HCMC (B) and HBimCl-$NbCl_5$/HCMC (C)

Figure 4 shows the catalyst particle size distribution before and after the carbonation at 170 °C. According to measurement results, the median particle size diameter of the fresh catalyst was larger than that of the spent catalyst. The particle size of catalyst with 50 vol. % of distribution (D50, median diameter) was 652 μm for fresh catalyst and 432 μm for spent catalyst. This could be explained by the mechanical breakdown by stirring during the carbonation reaction.

Figure 4. Particle size distributions of fresh catalyst (D) and spent catalyst at 170 °C (E) measured by Malvern Mastersizer 3000

The SEM spectra (Figure 5) indicates that the catalyst morphology changes after the carbonation reaction. No significant difference between the fresh catalyst and the first round recycled catalyst was noticed by the FTIR analysis (Figure S6), which has been pointed out over previous literature.[22] The content of $NbCl_5$ immobilized on the HBimCl-$NbCl_5$/HCMC was further examined by elemental analysis (Figure S3), which indicated that loss of niobium

occurred during the catalytic reaction due to the leaching of $NbCl_5$. The number of moles of $NbCl_5$ detected in per gram of catalyst was calculated from

$$\mathrm{n}'_{\mathrm{NbCl_5}}(\mathrm{mol.\,g^{-1}}) = \mathrm{n}'_{\mathrm{Nb}}(\mathrm{mol.\,g^{-1}}) = \frac{\mathrm{C_{Nb}}\cdot\mathrm{V_{sample}}}{\mathrm{M_{Nb}}\cdot\mathrm{m_{catalyst}}} \quad (16)$$

where, $\mathrm{n}'_{\mathrm{Nb}}$ is the number of moles of Nb in per gram of catalyst in mol.g^{-1}; $\mathrm{C_{Nb}}$ is the concentration of Nb detected by ICP-MS in mol.L^{-1}; V_{sample} is the total volume of measurement sample in L and $m_{catalyst}$ is the mass of the tested catalyst in g. In this work, the average number of moles of $NbCl_5$ immobilized on the fresh catalyst was characterized as 8.089×10^{-4} mol per gram of catalyst. Meanwhile, the carbon contents slightly increased after the catalytic reaction, because of the possible adsorption of the carbonated product on the surface of the catalyst.[22]

Figure 5. SEM images of fresh catalyst (A) and spent catalysts at 130 °C (B1), 150 °C (B2), 170 °C (B3)

Figure 6. TGA analyses for HCMC (F), fresh catalyst (G) and spent catalyst (H)

Figure 6 shows the TGA curves, representing a mass loss as a function of the temperature. for HCMC (F), fresh catalyst (G) and spent catalyst (H). The results revealed that fresh catalyst has lower initial weight loss temperature than that of HCMC at 220 °C and that of spent catalyst exceeding 220 °C. For this reason, the carbonation reaction was carried out below 220 °C.

3.2 Mass transfer study

During the carbonation reaction, the same reactor system was employed as described in the previous work.[34] We used the same methodology to estimate the mass transfer coefficient during the modeling stage (Table S1).

Henry's constant (Eq.(17)) and van't Hoff law (Eq.(18)) were used to estimate the absorption enthalpy of CO_2 in the FAME, EFAME and CFAME solutions

$$[\mathrm{CO_2}]^*_{\mathrm{liq}} = He \cdot P_{\mathrm{CO_2}} \quad (17)$$

$$\frac{He(T)}{He(T_{ref})} = exp\left(\frac{-\Delta H_{abs}}{R} \cdot \left(\frac{1}{T} - \frac{1}{T_{ref}}\right)\right) \quad (18)$$

where, *He* is Henry's constant in mol.L^{-1}.bar^{-1}; *P* is the CO_2 pressure in bar; $[CO_2]^*_{liq}$ is the solubility of CO_2 in the solution, mol.L^{-1}; *T* is the temperature in Kelvin, T_{ref} is the reference temperature, 130 °C, *R* is the gas constant, J.K^{-1}.mol^{-1} and ΔH_{abs} is the absorption enthalpy, J.mol^{-1}.

From Figure 7, it can be seen that the absorption enthalpies of CO_2 in FAME, EFAME and CFAME solutions are ΔH_{CFAME} = -13 345 J.mol^{-1}, ΔH_{EFAME} = -16 400 J.mol^{-1} and ΔH_{CFAME} = -14 627 J.mol^{-1}, respectively.

Figure 7. Van't Hoff curve for Henry's constants

A mass transfer study was performed in the absence of catalyst, thus the carbonation rate was equal to 0 mol.L^{-1}.s^{-1}.

3.3 Kinetic experiments

The effects of the reaction parameters such as the particle size distribution of the catalyst, the agitation speed, the reaction temperature and the catalyst loading on the carbonation kinetics were investigated.

3.3.1 Internal and external mass transfer

Three different stirring velocities (500, 1000 and 1500 rpm) were used in the carbonation experiments to reveal the effect of external mass transfer on the overall kinetics. Figure 8 compares the influence of different agitation speeds on the carbonation kinetics. The results indicate that the influence of the agitation speed is practically insignificant within the range 500-1500 rpm. Hence, experiments were performed using an agitation of 500 rpm.

Figure 8. Effect of agitation speed on the kinetics of carbonation reaction at 170 °C, 30 bar with $[EFAME]_{Initial}$= 2.61-2.99 mol.L^{-1}, native particle size of catalyst and catalyst loading=0.32 mol.L^{-1}

The conversion of the epoxide groups with the reaction time is plotted for different catalyst particle sizes in Figure 9. A significant increase in the reaction rate was observed with the decrease of particle size fraction from 500-355 µm to 125-63 µm. This could be explained by the larger reaction surface area available for epoxide groups and CO_2 when smaller catalyst particles are used. It was found that the kinetics of carbonation using the native particle size distribution is faster. This might be due to the fact that there is a significant fraction of particles with a diameter lower than 63 µm for experiments carried out with native particle size distribution.

Figure 9. Effect of the particle size distribution of catalyst on the kinetics of carbonation reaction at 170 °C, 30 bar with $[EFAME]_{Initial}$= 2.61-2.99 mol.L^{-1}, catalyst loading= 0.32 mol.L^{-1} and agitation speed of 500 rpm

3.3.2 Effect of reaction temperature

Figure 10 presents the effect of the reaction temperature (130, 150 and 170 °C) on the carbonation kinetics. As the temperature increases from 130 to 170 °C, the conversion rate of the epoxide group increases significantly. This accelerating temperature effect has also been mentioned in the literature.[38, 44]

Figure 10. Effect of reaction temperature on the kinetics of the carbonation reaction at 30 bar with $[EFAME]_{Initial}$= 2.61-2.99 mol.L^{-1}, native particle size of catalyst, catalyst loading= 0.32 mol.L^{-1} and agitation speed of 500 rpm

3.3.3 Effect of catalyst loading

Three different catalyst loadings (0, 0.42, 0.71 mol.L^{-1}) were investigated for the carbonation process. The experiments were performed at 170 °C. It can be seen that the carbonation

reaction with a higher catalyst loading is more rapid than the ones with a lower catalyst loading. The conversion reached a maximum of 90 % after 240 min (Figure 11).

Figure 11. Effect of catalyst loading amount on the kinetics of carbonation reaction at 170 °C, 30 bar with $[EFAME]_{Initial}$= 2.61-2.99 mol.L^{-1}, native particle size of catalyst and agitation speed of 500 rpm

3.4 Characterization of carbonated products

FTIR spectra of the EFAME before carbonation reaction and CFAME after 23 hours of reaction at 170 °C and 30 bar are displayed in Figure S7 in the Supporting Information. After the carbonation, the peaks at 842 cm^{-1}, 821 cm^{-1}, which are attributed to the epoxide group (C-O-C) stretch, disappeared, while a new peak was observed at 1807 cm^{-1} due to the carboxylic group (C=O) stretch of the carbonate group.

3.5 Kinetic model

Figure 12 shows an example of the model fitting to the experimental data for Exp 2. One can notice that the model prediction is lower than the experimental concentrations after 300 minutes. This difference might be due to the fact that the model did not consider the slight catalyst deactivation. The experimental data shows an induction period in the first 90min. As mentioned in the previous work,[37] this phenomenon might be due to the reaction conditions (low catalyst loading and low reaction pressure) and the structural features (limited active sites) of the catalyst. The reaction substrate has not been previously allosterically controled by the catalytic site, and the potential nonspecific binding of the reaction mediums to the catalyst may result in restrict availability of the epoxide group to the catalyst's active site during the reaction.

Figure 13 displays the overall parity plot of the experimental data and the simulated values. From this figure, one can notice that the proposed kinetic model could simulate the experimental data. The coefficient of determination was equal to 96.4 %, showing the good reliability of the model.

Figure 12. Fitting of the model to the experimental data for Exp 2

Figure 13. Overall parity plot of experimental versus simulated values for the epoxide value

Table 3 gives the estimated and statistical data for the carbonation of EFAME with HbimCl-$NbCl_5$/HCMC.

Table 3 Estimated And Statistical Data At T_{ref} = 150 °C For The Carbonation Of EFAME

4. Conclusions

A heterogeneous catalyst HBimCl-$NbCl_5$/HCMC was synthesized and characterized for the carbonation of epoxidized fatty acid methyl esters originating from cottonseed oil. The carbonation reaction of epoxidized fatty acid methyl ester was carried out effectively in a laboratory-scale autoclave by using HBimCl-$NbCl_5$/HCMC as the catalyst under isothermal and isobaric conditions. The effects of external and internal mass transfer were found out to be negligible on the carbonation reaction. The carbonation kinetics were enhanced by increasing the reaction temperature from 130 to 170 °C. A kinetic model was proposed to simulate the carbonation process and kinetic constants were estimated with nonlinear regression analysis. We conclude that HBimCl-$NbCl_5$/HCMC can be used as a heterogeneous catalyst for the carbonation reaction. However, more investigations on the catalyst deactivation need to be carried out to improve the catalyst reusability.

Notation

Carb	carbonated group
Ep	epoxidized group
DB	double bond
Cat.	catalyst
He	Henry's constant [mol.L^{-1}.bar^{-1}]
ΔH	absorption enthalpy [J.mol^{-1}]
I1, I2, I3	intermediates 1, 2, 3
r	rate of formation or disappearance of intermediate [mol.L^{-1}.s^{-1}]
P	pressure [bar]
R	reaction rate [mol.L^{-1}.s^{-1}]
R	gas constant [J.K^{-1}.mol^{-1}]
R^2	coefficient of explanation [%]
T	temperature [°C]
y_i	experimental observable
$\bar{y}$	mean value of the experimental observables
$\hat{y}_i$	observable simulated by the model
$[\mathrm{CO_2}]_{\mathrm{liq}}$	solubility of CO_2 in the solution [mol.L^{-1}]
$[\mathrm{CO_2}]^*_{\mathrm{liq}}$	equilibrium concentration of CO_2 in the gas-liquid phase [mol.L^{-1}]
n^*_{liq}	moles of CO_2 in the solution [mol]
n_{liq}	moles of CO_2 in the solution [mol]
$N_{\mathrm{CO_2}}$	interfacial component flux [mol.m^{-2}.s^{-1}]
k_L	mass transfer coefficient of CO_2 in the solution
a	ratio of surface area of gas-liquid mass transfer to volume [m^{-1}]
(k_L.*a*)'	modified volumetric mass transfer coefficient [(K.Pa^{-1}.s^{-1}) $^{-0.5}$. (kg.m^{-3}. Pa^{-1}.s^{-1}) $^{-0.25}$.s^{-1}]
D50	median diameter [µm]

Subscripts and superscripts

Carbonation	carbonation reaction
liq	liquid
org	organic
ref	reference
i	component i

Greek letters

f	objective function
θ^2	coefficient of determination

Abbreviation

TEAB	tetraethylammonium bromide
HCMC	protonated carboxymethyl cellulose
HBimCl	1-hydroxypropyl-3-n-butylimidazolium chloride
FAME	fatty acid methyl ester
EFAME	epoxidized fatty acid methyl ester
CFAME	carbonated fatty acid methyl ester

Acknowledgments

This work is part of the activities at the Johan Gadolin Process Chemistry Centre (PCC) and financed by Academy of Finland, the Academy Professor grants 319002 (T. Salmi) and 320115 (P. Tolvanen). The authors express their gratitude to Rose-Marie Latonen for her technical assistance for the FTIR analysis. The authors thank the China Scholarship Council: Co-operation Program with the UTs and INSAs (France). The authors thank the Johan Gadolin Scholarship Program provided by Johan Gadolin Process Chemistry Centre (PCC) at Åbo Akademi University.

Data Availability Statement

Data available on request from the authors. The data that support the findings of this study are available from the corresponding author upon reasonable request.

Supporting Information

The Supporting Information is available free of charge: reaction mechanisms for the titration of oxirane and double bond; calculation method of carboxyl group content in protonated carboxymethyl cellulose; preparation mechanism and characterization of HBimCl; results of elemental analysis and FTIR analysis of catalyst; details of the modeling results.

References

[1] Whitmarsh L. What's in a name? Commonalities and differences in public understanding of "climate change" and "global warming". *Public Underst Sci*. 2009;18:401–420.

[2] Lashof DA, Ahuja DR. Relative contributions of greenhouse gas emissions to global warming, *Nature*. 1990;344:529–531.

[3] Aresta M, Dibenedetto A, Angelini A. Catalysis for the valorization of exhaust carbon: From CO_2 to chemicals, materials, and fuels. Technological use of CO_2. *Chem Rev*. 2014;114:1709–1742.

[4] Kim I, Yi MJ, Byun SH, Park DW, Kim BU, Ha CS. Biodegradable polycarbonate synthesis by copolymerization of carbon dioxide with epoxides using a heterogeneous zinc complex. *Macromol Symp*. 2005; 224:181–192.

[5] Bähr M, Mülhaupt R. Linseed and soybean oil-based polyurethanes prepared via the non-isocyanate route and catalytic carbon dioxide conversion. *Green Chem*. 2012;14:483–489.

[6] Rokicki G, Parzuchowski PG, Mazurek M. Non-isocyanate polyurethanes: Synthesis, properties, and applications. *Polym Adv Technol*. 2015;26:707–761.

[7] Besse V, Camara F, Voirin C, AuvergneR, Caillol S, Boutevin B. Synthesis and applications of unsaturated cyclocarbonates. *Polym Chem*. 2013;4:4545–4561.

[8] Blattmann H, Fleischer M, Bähr M, Mülhaupt R. Isocyanate- and phosgene-free routes to polyfunctional cyclic carbonates and green polyurethanes by fixation of carbon dioxide. *Macromol Rapid Commun*. 2014;35:1238–1254.

[9] Figovsky O, Shapovalov L, Karchevsky V, Loelovich M. Development of environmentally friendly polymeric materials. *J Sci Eng B*. 2005;2:266–275.

[10] Jr DB, Kumpf RJ. Method for modifying the backbone of polymeric resins. US5605979A, 1997. https://patents.google.com/patent/US5605979A/en (accessed April 2, 2019).

[11] Pérez-Sena WY, Cai X, Kebir N, Vernières-Hassimi L, Serra C, Salmi T, Leveneur S. Aminolysis of cyclic-carbonate vegetable oils as a non-isocyanate route for the synthesis of polyurethane: A kinetic and thermal study. *Chem Eng J.* 2018;346:271–280.

[12] Poussard L, Mariage J, Grignard B, Detrembleur C, Jérôme C, Calberg C, Heinrichs B, De Winter J, Gerbaux P, Raquez JM, Bonnaud L, Dubois P. Non-Isocyanate polyurethanes from carbonated soybean oil using monomeric or oligomeric diamines to achieve thermosets or thermoplastics. *Macromolecules*. 2016;49:2162–2171.

[13] Lligadas G, Ronda JC, Galià M, Cádiz V. Renewable polymeric materials from vegetable oils: A perspective. *Mater Today*. 2013;16:337–343.

[14] Liu W, Lu G, Xiao B, Xie C. Potassium iodide–polyethylene glycol catalyzed cycloaddition reaction of epoxidized soybean oil fatty acid methyl esters with CO_2. *RSC Adv*. 2018;8:30860–30867.

[15] Li Z, Zhao Y, Yan S, Wang X, Kang M, Wang J, Xiang H. Catalytic synthesis of carbonated soybean oil. *Catal Lett*. 2008;123:246–251.

[16] Bobbink FD, Dyson PJ. Synthesis of carbonates and related compounds incorporating CO_2 using ionic liquid-type catalysts: State-of-the-art and beyond. *J Catal.* 2016;343:52–61.

[17] Narra N, Rachapudi BNP, Vemulapalli SPB, Korlipara PV. Lewis-acid catalyzed synthesis and characterization of novel castor fatty acid-based cyclic carbonates. *RSC Adv*. 2016;6:25703–25712.

[18] Büttner H, Steinbauer J, Wulf C, Dindaroglu M, Schmalz HG, Werner T. Organocatalyzed synthesis of oleochemical carbonates from CO_2 and renewables. ChemSusChem. 10 (6) (2017) 1076–1079.

[19] Desens W, Werner T. Convergent activation concept for CO_2 fixation in carbonates. *Adv Synth Catal*. 2016;358:622–630.

[20] Babu R, Kim SH, Kathalikkattil AC, Kuruppathparambil RR, Kim DW, Cho SJ, Park DW. Aqueous microwave-assisted synthesis of non-interpenetrated metal-organic framework for room temperature cycloaddition of CO_2 and epoxides. *Appl Catal Gen*.2017;544:126–136.

[21] Wang J, Zhao Y, Li Q, Yin N, Feng Y, Kang M, Wang X. Pt doped $H_3PW_{12}O_{40}/ZrO_2$ as a heterogeneous and recyclable catalyst for the synthesis of carbonated soybean oil. *J Appl Polym Sci*. 2012;124:4298–4306.

[22] Wu X, Wang M, Xie Y, Chen C, Li K, Yuan M, Zhao X, Hou Z. Carboxymethyl cellulose supported ionic liquid as a heterogeneous catalyst for the cycloaddition of CO_2 to cyclic carbonate. *Appl Catal Gen*. 2016;519:146–154.

[23] Guo F. A novel 2D Cu(II)-MOF as a heterogeneous catalyst for the cycloaddition reaction of epoxides and CO_2 into cyclic carbonates. *J Mol Struct*. 2019;1184:557–561.

[24] Onyenkeadi V, Aboelazayem O, Kellici S, Saha B. Greener synthesis of butylene carbonate via CO_2 utilisation using graphene-inorganic nanocomposite catalysts, in: Toulouse, France, 2018. http://researchopen.lsbu.ac.uk/2334/ (accessed December 3, 2018).

[25] Léonard GLM, Belet A, Grignard B, Calberg C, Gilbert B, Jérôme C, Heinrichs B. Heterogenization of a cyclocarbonation catalyst: Optimization and kinetic study. *Catal Today*. 2019;334:140–155.

[26] Klemm D, Heublein B, Fink HP, Bohn A. Cellulose: Fascinating biopolymer and sustainable raw material. *Angew Chem Int Ed*. 2005;44:3358–3393.

[27] Gamelas JAF, Oliveira F, Evtyugina MG, Portugal I, Evtuguin DV. Catalytic oxidation of formaldehyde by ruthenium multisubstituted tungstosilicic polyoxometalate supported on cellulose/silica hybrid. *Appl Catal Gen*. 2016;509:8–16.

[28] Reddy KR, Kumar NS. Cellulose-supported copper(0) catalyst for aza-Michael addition. *Synlett*. 2006;2006:2246–2250.

[29] Zhou Z, Lu C, Wu X, Zhang X. Cellulose nanocrystals as a novel support for CuO nanoparticles catalysts: Facile synthesis and their application to 4-nitrophenol reduction. *RSC Adv*. 2013;3:26066–26073.

[30] Roshan KR, Mathai G, Kim J, Tharun J, Park GA, Park DW. A biopolymer mediated efficient synthesis of cyclic carbonates from epoxides and carbon dioxide. *Green Chem*. 2012;14:2933–2940.

[31] Sun J, Wang J, Cheng W, Zhang J, Li X, Zhang S, She Y. Chitosan functionalized ionic liquid as a recyclable biopolymer-supported catalyst for cycloaddition of CO_2. *Green Chem.* 2012;14:654–660.

[32] Tharun J, Kim DW, Roshan R, Hwang Y, Park DW. Microwave assisted preparation of quaternized chitosan catalyst for the cycloaddition of CO_2 and epoxides. *Catal Commun*. 2013;31:62–65.

[33] Gui X, Chen S, Yun Z. Continuous production of biodiesel from cottonseed oil and methanol using a column reactor packed with calcined sodium silicate base catalyst. *Chin J Chem Eng*. 2016;24:499–505.

[34] Cai X, Matos M, Leveneur S. Structure–Reactivity: Comparison between the carbonation of epoxidized vegetable oils and the corresponding epoxidized fatty acid methyl ester. *Ind Eng Chem Res.* 2019;58:1548–1560.

[35] Maerker G. Determination of oxirane content of derivatives of fats. *J Am Oil Chem Soc.* 1965;42:329–332.

[36] Paquot C. Standard methods for the analysis of oils, fats and derivatives. Elsevier, Amsterdam, 2013.

[37] Cai X, Zheng JL, Wärnå J, Salmi T, Taouk B, Leveneur S. Influence of gas-liquid mass transfer on kinetic modeling: Carbonation of epoxidized vegetable oils. *Chem Eng J*. 2017;313:1168–1183.

[38] Haario H. MODEST-User's Guide, Profmath Oy, Helsinki, 2001.

[39] Leis JR, Kramer MA. Algorithm 658: ODESSA–an ordinary differential equation solver with explicit simultaneous sensitivity analysis. *ACM Trans Math Softw*. 1988;14:61–67.

[40] Spendley W, Hext GR, Himsworth FR. Sequential application of simplex designs in optimisation and evolutionary operation. *Technometrics*. 1962;4:441–461.

[41] Marquardt D, An algorithm for least-squares estimation of nonlinear parameters. *J Soc Ind Appl Math*. 1963;11:431–441.

[42] Yildiz M, Alp S, Saltan F, Akat H. Synthesis of new imidazole-based monomer and copolymerization studies with methyl methacrylate. *Iranian Polym J.* 2020;29:515–523.

[43] Bouamoud R, Mulongo-Masamba R, Hamidi AE, Halim M, Arsalane S. Structural assessments of kerogen-rich oil shale from the Central Kongo formation by solid-state 13 C nuclear magnetic resonance and thermal processes. *J Therm Anal Calorim.* 2021;3:1–12.

[44] Polettini A, Pomi R, Stramazzo A. CO_2 sequestration through aqueous accelerated carbonation of BOF slag: A factorial study of parameters effects. *J Environ Manage*. 2016;167:185–195.

Table 1 Experimental matrix for kinetic modeling

Exp	Nature of organic phase	$[Ep]_{org}$ / mol.L^{-1}	$[DB]_{org}$ / mol.L^{-1}	$[Cat.]_0$[a] / mol.L^{-1}	P_{CO2} / bar	T / °C	Agitation speed / rpm
1	EFAME	2.30	0.914	0.37	30.00	130	500
2	EFAME	2.40	0.839	0.71	30.09	170	500
3	EFAME	2.56	0.737	0.61	29.70	170	500
4	EFAME	2.52	0.914	0.34	30.00	150	500
5	EFAME	2.17	1.223	0.39	30.00	170	500

[a] Catalyst loading (mol.L^{-1}) = mass of catalyst in grams $\times$ 8.089 $\times$ 10^{-4} mol of $NbCl_5$ per gram of catalyst. 0.0008089 is the number of moles of $NbCl_5$ detected in per gram of fresh catalyst by ICP-MS.

Table 2 Experimental matrix for mass transfer modeling with initial concentrations

Exp	$P_{reactor}$ / bar	$T_{reactor}$ / °C	FAME / wt. %	EFAME / wt. %	CFAME / wt. %	Agitation speed / rpm
6	30	130	50	50	0	500
7	30	150	50	50	0	500
8	30	170	50	50	0	500
9	30	130	0	0	100	500
10	30	150	0	0	100	500
11	30	170	0	0	100	500
12	30	130	0	100	0	500
13	30	150	0	100	0	500
14	30	170	0	100	0	500
15	30	150	100	0	0	500
16	30	170	100	0	0	500

Table 3 Estimated and statistical data at T_{ref} = 150 °C for the carbonation of EFAME

	Estimated	Standard error	Standard error %
$(k_{carbonation})_{EFAME}$ / $L^2.mol^{-2}.s^{-1}$	0.251×10^{-2}	0.952×10^{-3}	37.9
$(Ea_{carbonation})_{EFAME}$ / $J.mol^{-1}$	100 000	6980	7.0
α / $L.mol^{-1}$	1.17	0.621	53.0

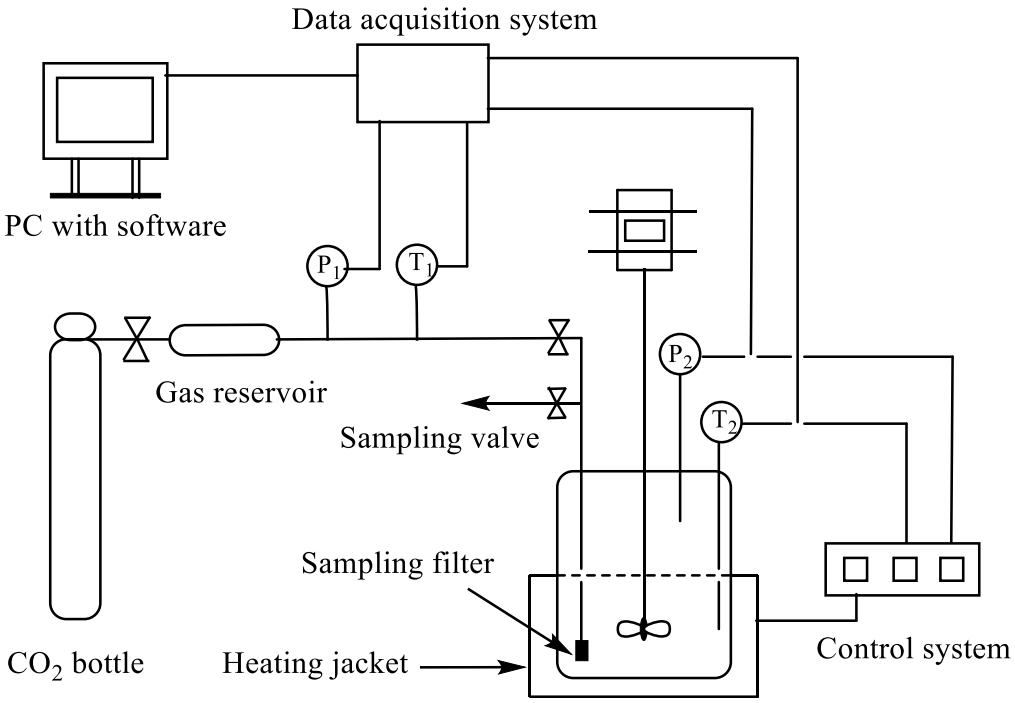

Fig.1. Simplified scheme of the reaction setup.

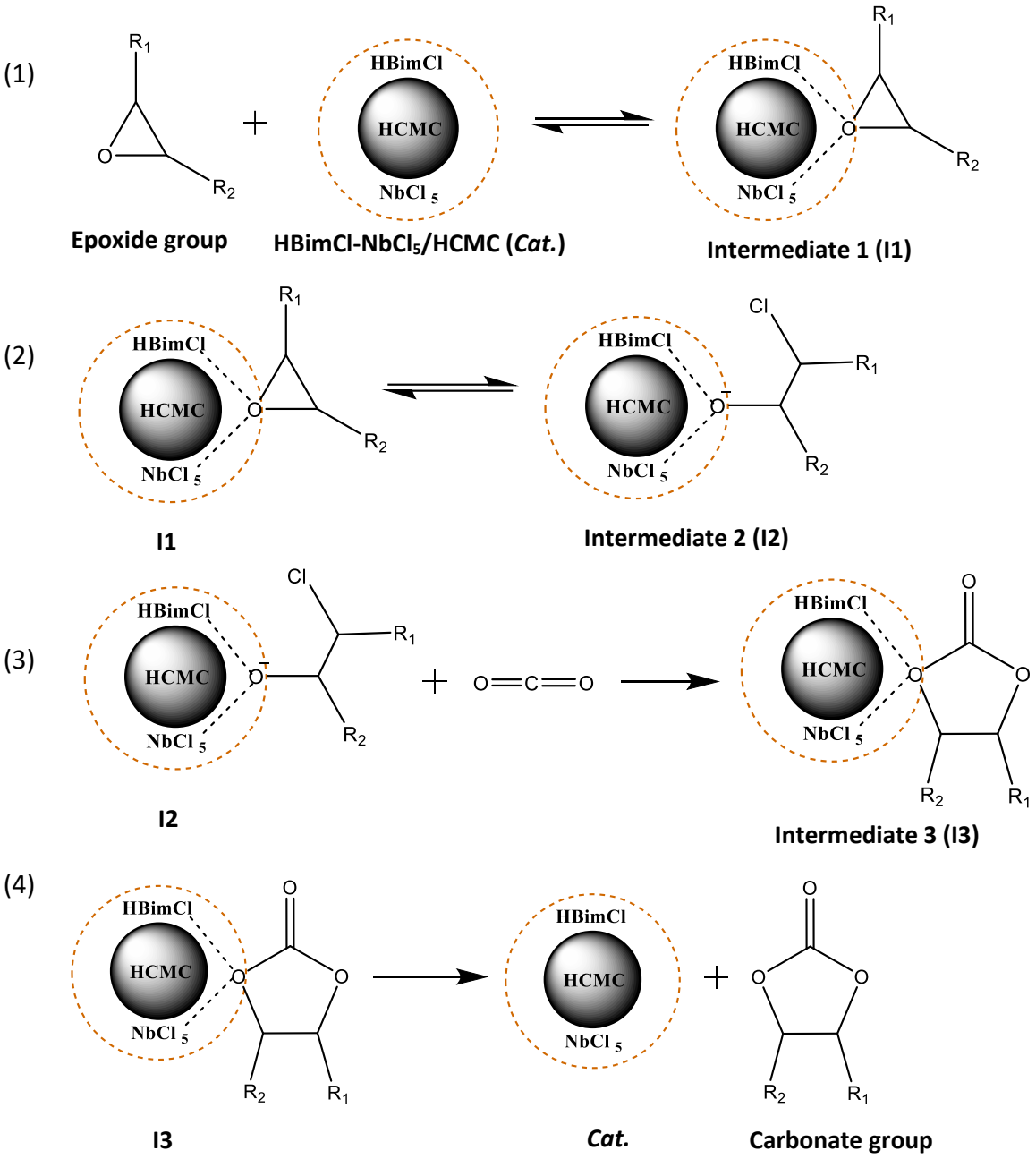

Fig.2. Simplified mechanism of carbonation of EFAME by HBimCl-$NbCl_5$/HCMC.

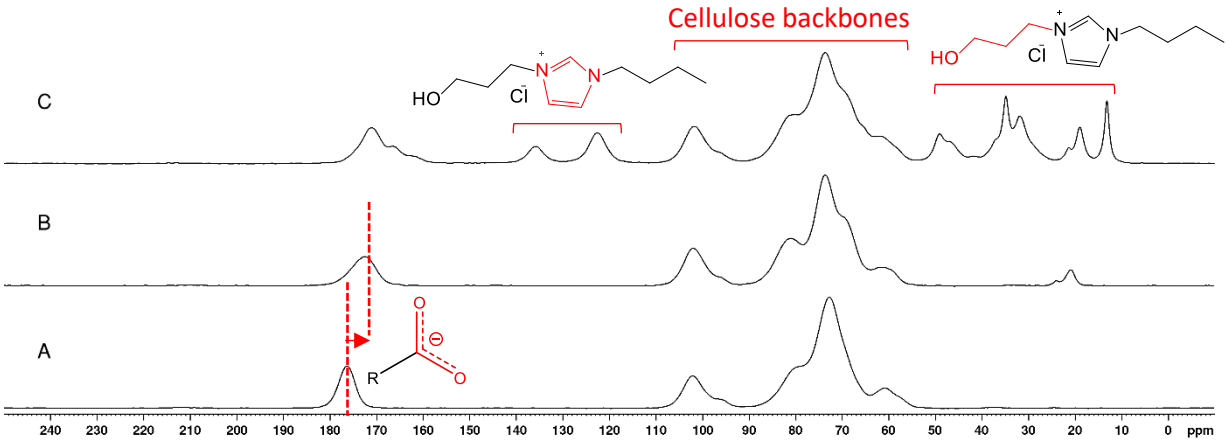

Fig.3. ^{13}C CP-MAS spectra of NaCMC (A), HCMC (B) and HBimCl-$NbCl_5$/HCMC (C).

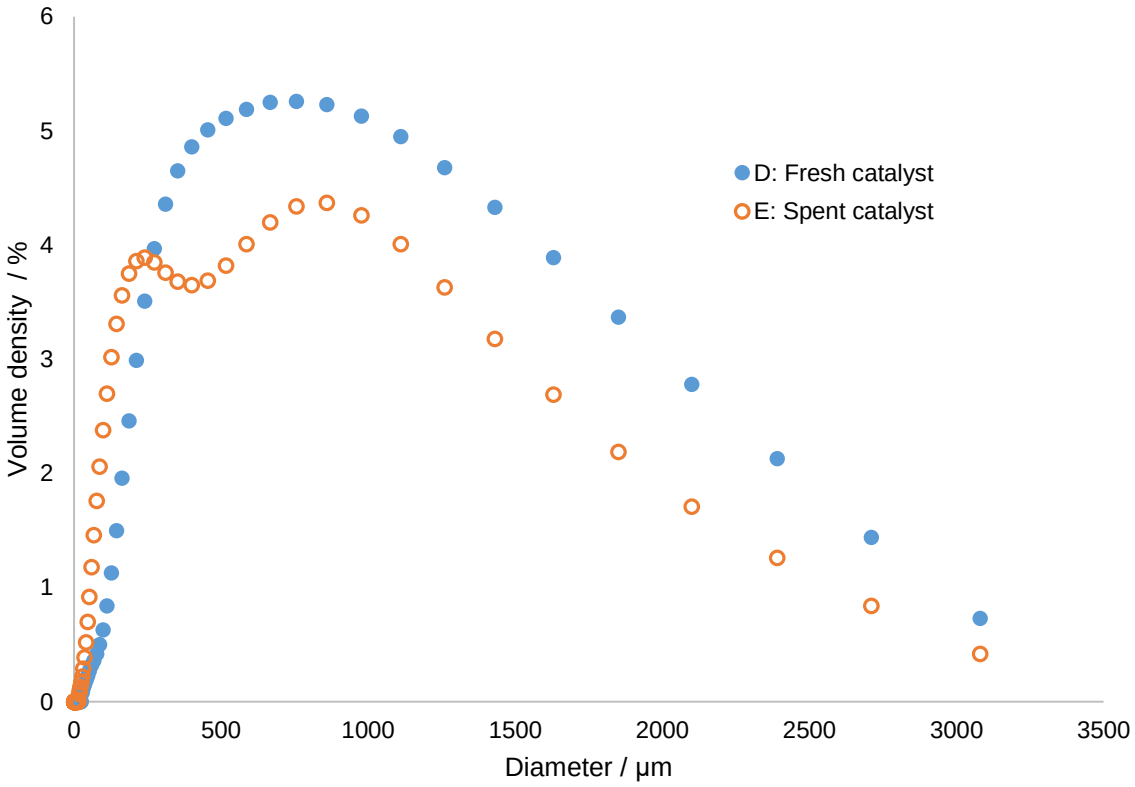

Fig.4. Particle size distributions of fresh catalyst (D) and spent catalyst at 170 °C (E) measured by Malvern Mastersizer 3000.

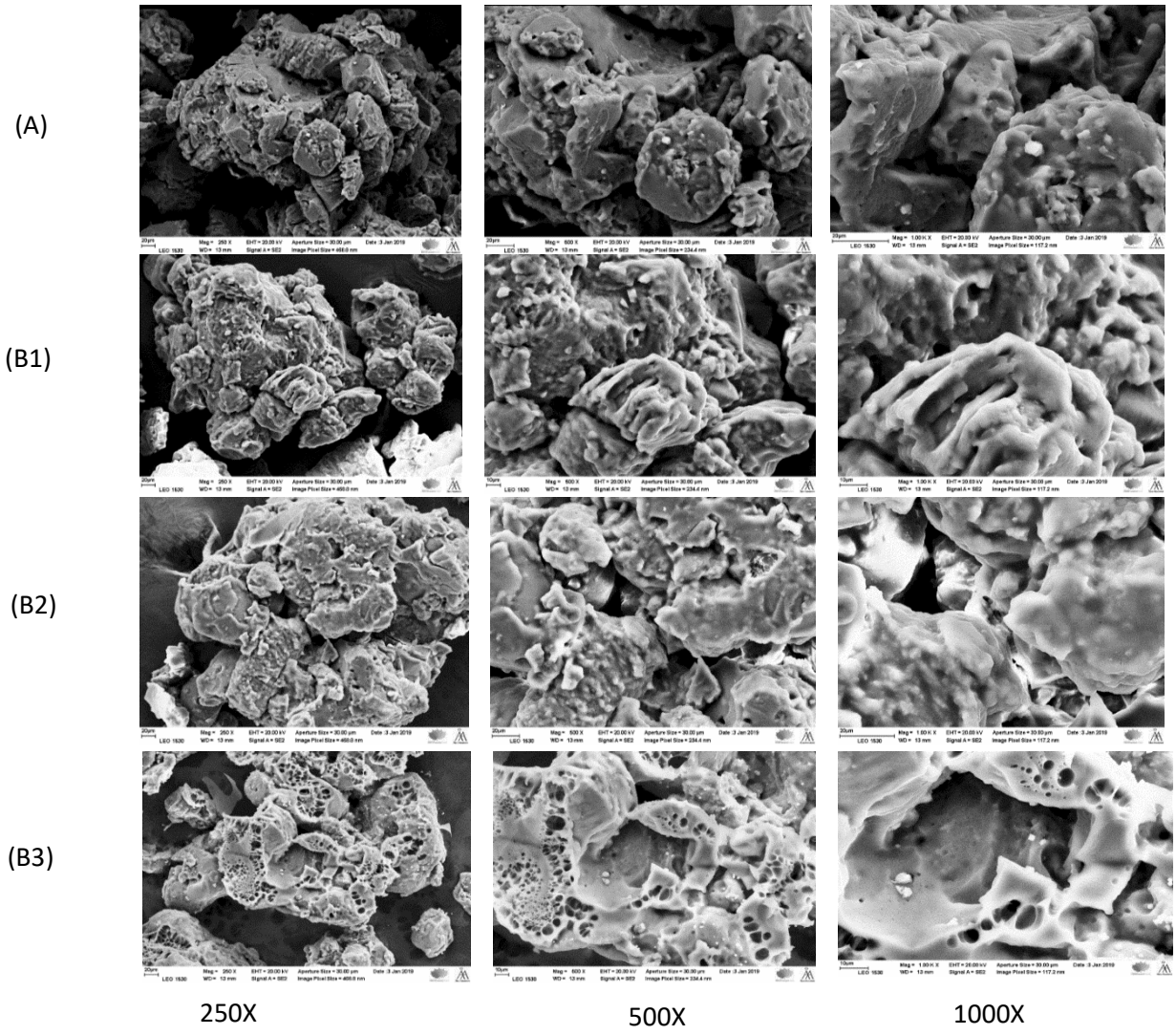

Fig.5. SEM images of fresh catalyst (A) and spent catalysts at 130 °C (B1), 150 °C (B2), 170 °C (B3).

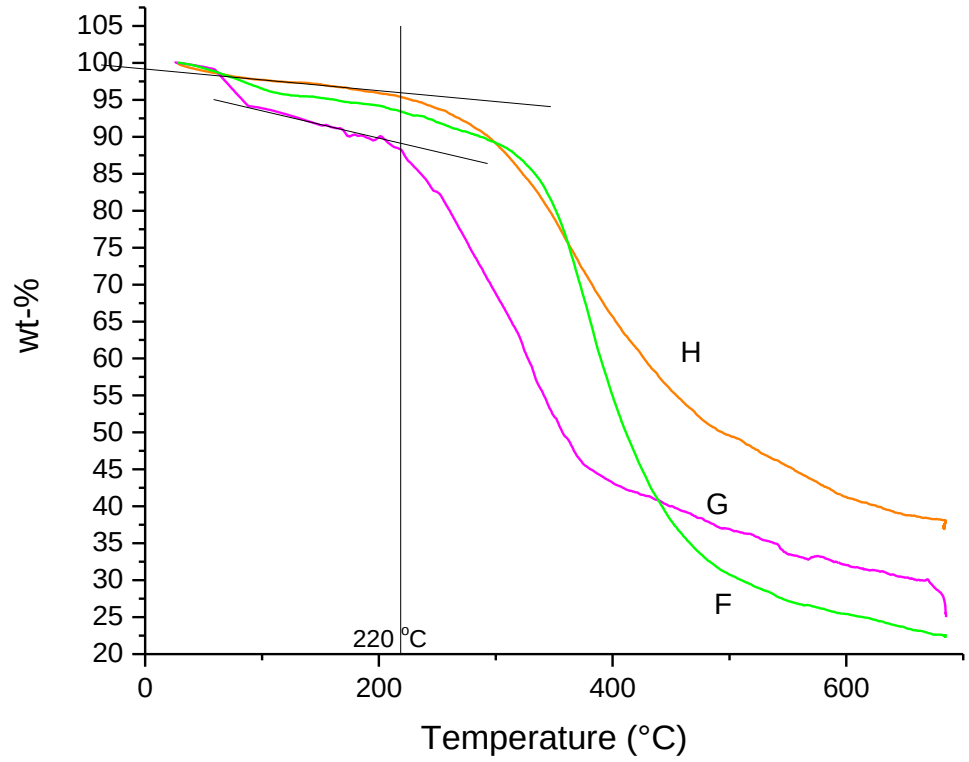

Fig.6. TGA analyses for HCMC (F), fresh catalyst (G) and spent catalyst (H).

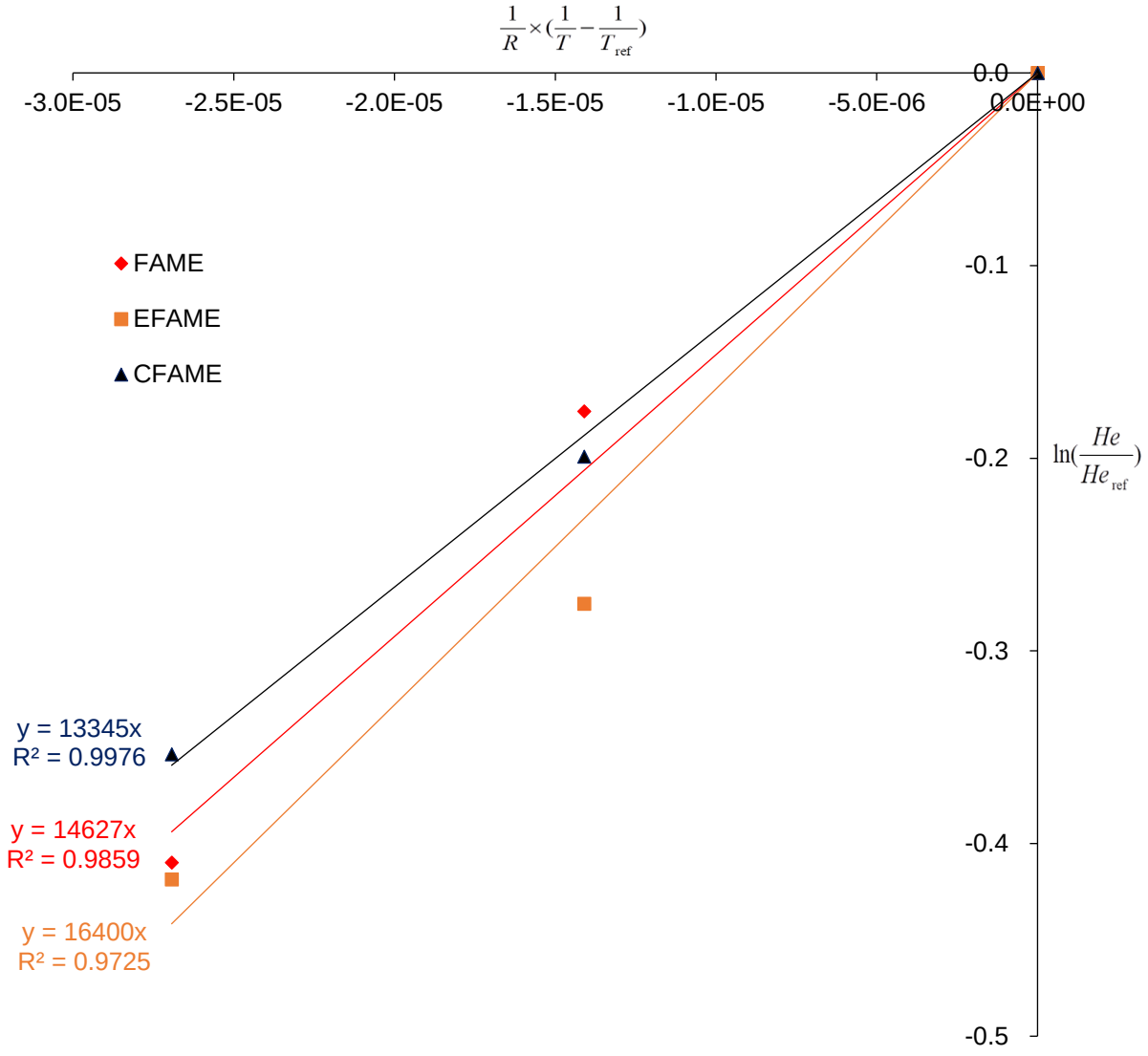

Fig.7. Van't Hoff curve for Henry's constants.

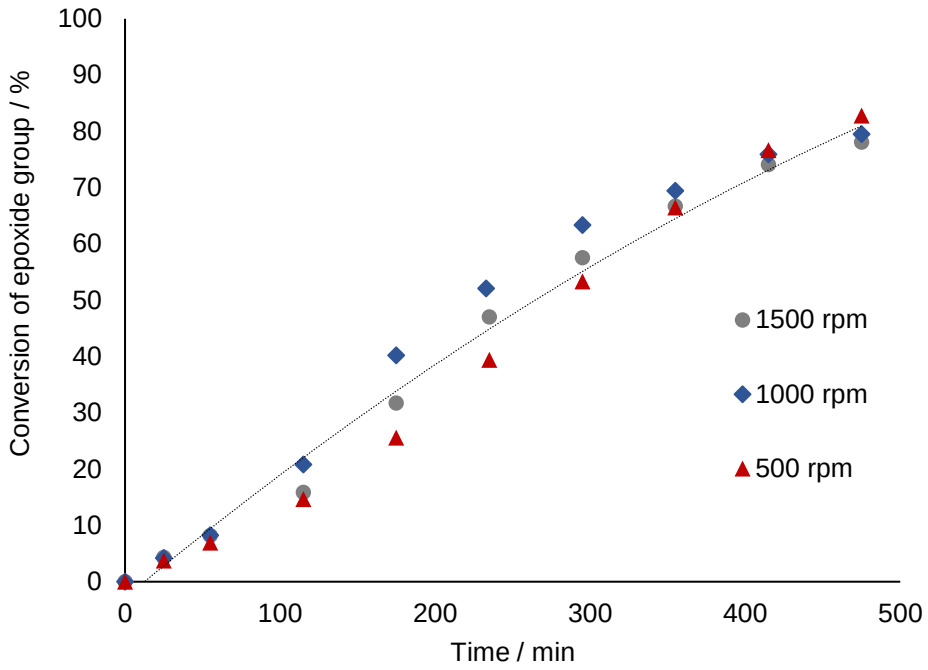

Fig.8. Effect of agitation speed on the kinetics of carbonation reaction at 170 °C, 30 bar with $[EFAME]_{Initial}$= 2.61-2.99 mol.L^{-1}, native particle size of catalyst and catalyst loading=0.32 mol.L^{-1}.

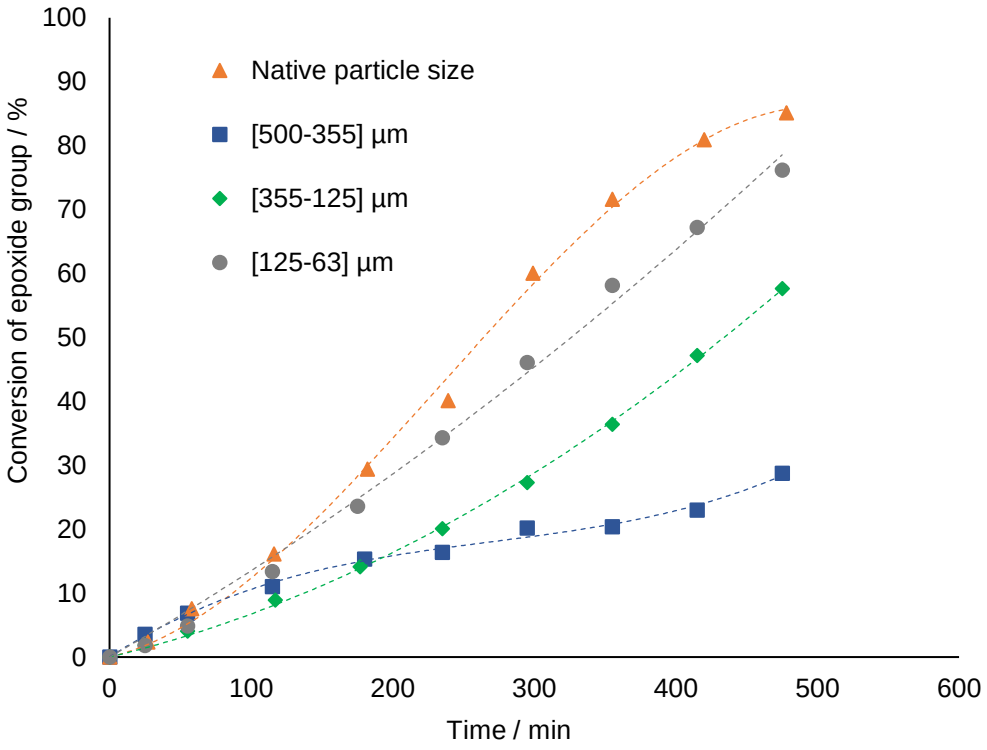

Fig.9. Effect of the particle size distribution of catalyst on the kinetics of carbonation reaction at 170 °C, 30 bar with $[EFAME]_{Initial}$= 2.61-2.99 mol.L^{-1}, catalyst loading= 0.32 mol.L^{-1} and agitation speed of 500 rpm.

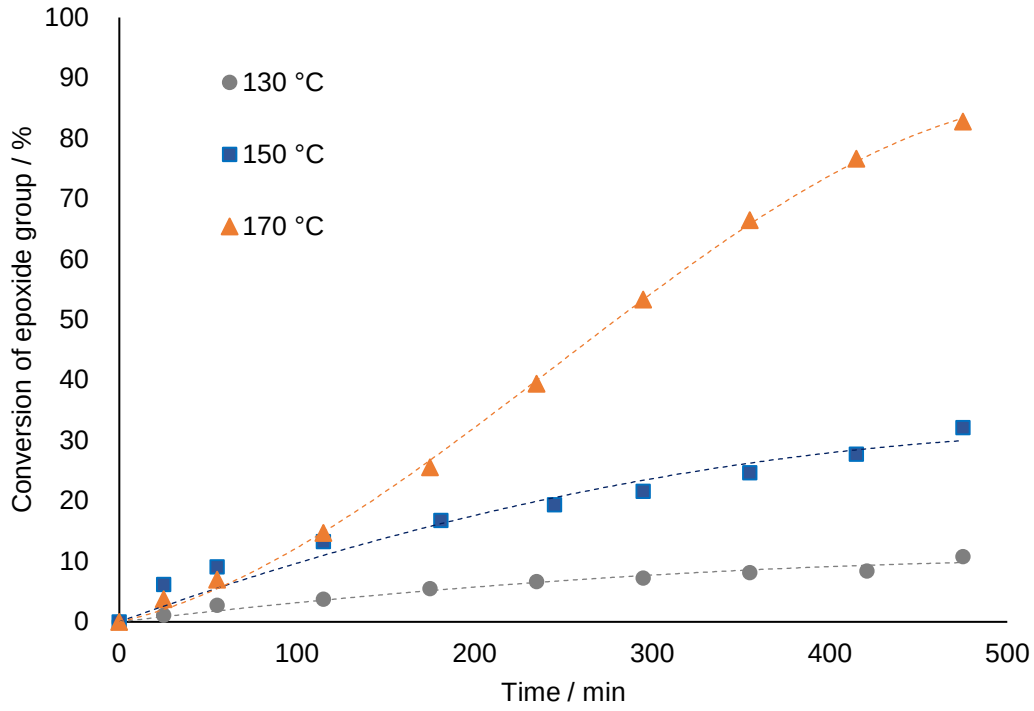

Fig.10. Effect of reaction temperature on the kinetics of the carbonation reaction at 30 bar with $[EFAME]_{Initial}$= 2.61-2.99 mol.L^{-1}, native particle size of catalyst, catalyst loading= 0.32 mol.L^{-1} and agitation speed of 500 rpm.

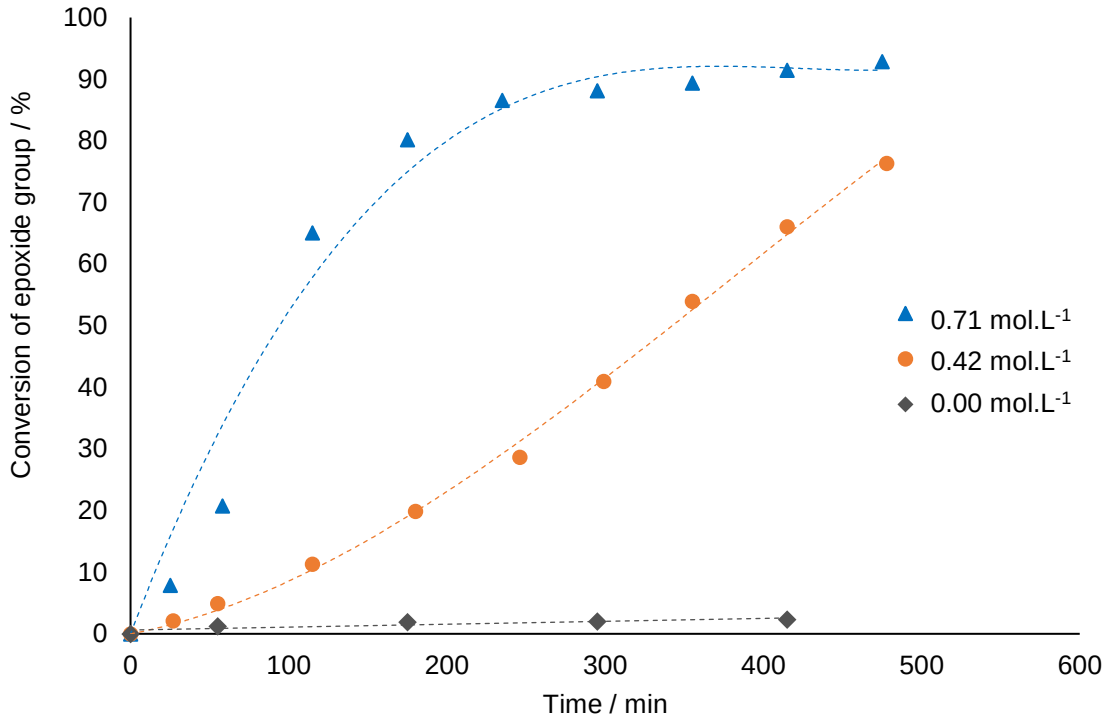

Fig.11. Effect of catalyst loading amount on the kinetics of carbonation reaction at 170 °C, 30 bar with $[EFAME]_{Initial}$= 2.61-2.99 mol.L^{-1}, native particle size of catalyst and agitation speed of 500 rpm.

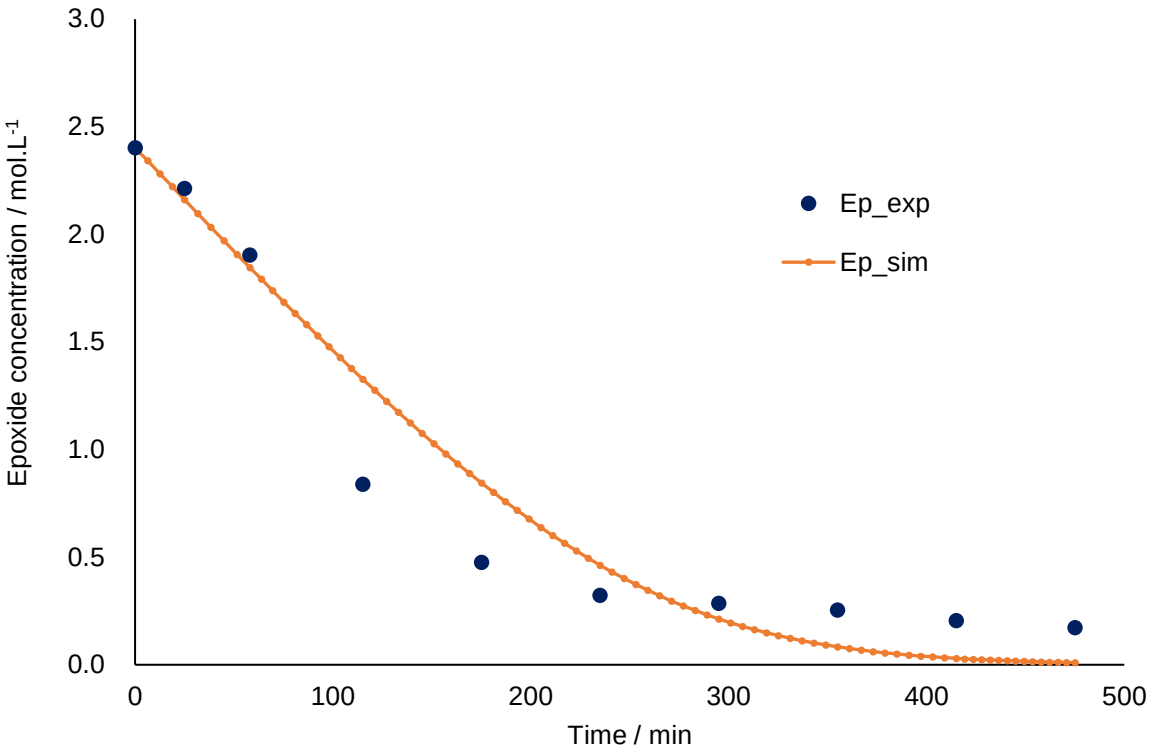

Fig.12. Fitting of the model to the experimental data for Exp 2.

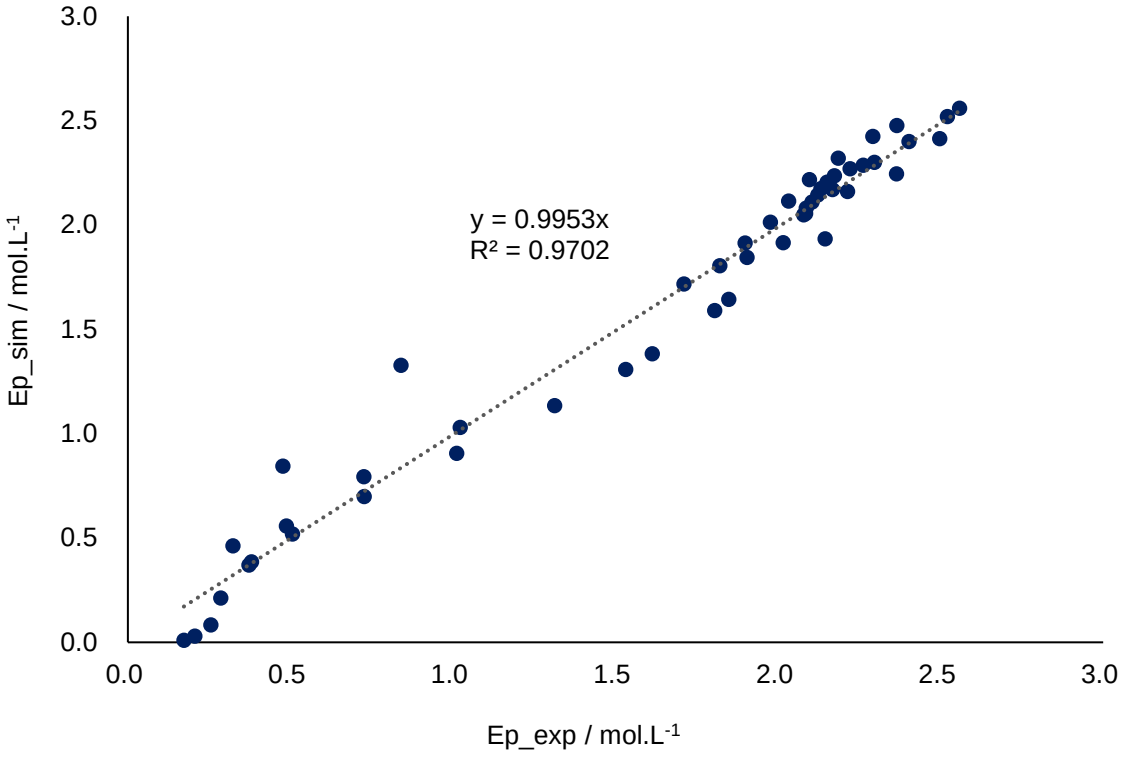

Fig.13. Overall parity plot of experimental versus simulated values for the epoxide value.